



Revisiting the scalar leptoquark (S_1) model with the updated leptonic constraints

Bibhabasu De^a

Department of Physics, The ICFAI University Tripura, Kamalghat, Tripura 799210, India

Received: 8 October 2023 / Accepted: 21 November 2023 / Published online: 30 November 2023
© The Author(s) 2023

Abstract The Standard Model, if extended to the energy scale of $\mathcal{O}(1)$ TeV, the known particle spectrum could be augmented with a scalar leptoquark. Within this minimally extended framework, explaining the anomalous magnetic moment and electric dipole moment simultaneously for the three lepton generations over a parameter space consistent with all the lepton flavor violating bounds is possible. Such a model can be tested or falsified through the collider search experiments and/or by probing the low-energy lepton phenomena. This work studies the current prospects of the model in the presence of recent experimental updates for the leptonic observables.

1 Introduction

The Standard Model (SM) has already explained the color and electroweak sectors up to a high degree of testable precision. Further, the discovery of the 125 GeV Higgs boson at the Large Hadron Collider (LHC) has completed the proposed particle spectrum of the SM [1, 2]. However, certain experimental observations and theoretical issues can't be explained within the framework of the SM and thus indicate the presence of some New Physics (NP) yet to be explored. For example, the idea of gauge coupling unification hints at a more fundamental theory corresponding to a single gauge group. The SM gauge group, i.e., $SU(3)_C \times SU(2)_L \times U(1)_Y$ can be considered as its effective low-energy version obtained via a particular symmetry-breaking chain. The list of such Grand Unified Theories (GUT) includes $SU(4)$ [3], $SU(5)$ [4], $SO(10)$ [5, 6], E_6 [7, 8], etc. It is interesting to note that within a GUT structure, quarks and leptons can directly couple at the tree-level through a hypothetical mediator – Leptoquark (LQ) (for recent reviews, see Refs. [9–12]). Though, in principle, within a local quantum field theory LQs can either

be scalar or vector, the scalar LQs are more useful to study the loop-induced Beyond Standard Model (BSM) contributions [13–15]. LQs are crucial from various phenomenological aspects. For example, an extension of the SM with a LQ can explain several B-meson anomalies [16–26] or can contribute to the flavor violating processes like $\tau \rightarrow \mu\gamma$ and $h \rightarrow \tau\mu$ [27]. LQs may also be significant for the dark matter phenomenology [28–30] and the production of scalar particles at the LHC [31–35]. Note that the simplest GUT extensions assume a heavy LQ [36, 37] to evade the proton lifetime constraints, but they can't be produced at the LHC. However, there are GUT formulations that can explain the stability of proton with a TeV-scale scalar LQ [38–43]. Thus, in this paper, the later GUT motivation will be considered as the gauge theoretical background for the new interactions, i.e., the SM will be extended to an energy scale of $\mathcal{O}(1)$ TeV to augment the observed particle spectrum with a scalar LQ.

Recent experiments have resulted in some remarkable observations in the lepton sector, which may indicate towards a possible BSM theory yet to be discovered. For example, in 2021 a combined result from the Fermilab-based Muon $g-2$ collaboration and Brookhaven National Laboratory (BNL) showed a 4.2σ discrepancy between the predicted and measured values of the anomalous magnetic moment of muon [44, 45]. The result has been updated very recently on August 2023, enhancing the significance to 5σ [46].¹ Moreover, a precision measurement of the fine-structure constant using either Cesium (Cs) [50] or Rubidium (Rb) [51] indicates a similar anomaly in $(g-2)_e$. However, note that a relative sign between the two results leads to an experimental dispute that

¹ A recent lattice calculation of the hadronic vacuum polarization (HVP) term by the BMW collaboration [47] and a preliminary experimental update from the CMD-3 detector [48] indicate a significant tension with the present data which may result in a smaller and less significant discrepancy [49] between the predicted and observed values of $(g-2)_\mu$.

^a e-mail: bibhabasude@gmail.com (corresponding author)

can't be settled with the present technologies. LQs can play a vital role in explaining the discrepancy in $(g - 2)_\mu$ [52–58]. Moreover, in the presence of a scalar LQ, various NP signatures, e.g., the neutrino oscillation, W mass anomaly, lepton flavor violating decays and dark matter can be connected to the $(g - 2)_{e, \mu}$ anomalies within a single BSM formulation [29, 59, 59–67]. LQs can also have important implications to explain the electric dipole moment (EDM) of leptons [68–70].

In this paper, a *minimal* extension of the SM has been considered with a scalar LQ $S_1(\bar{\mathbf{3}}, \mathbf{1}, 1/3)$ at an energy scale of $\mathcal{O}(1)$ TeV. In Refs. [66, 71], it has already been studied in detail that such a simple BSM framework can easily explain all the possible NP signatures and experimental constraints in the lepton sector. However, we shall see that the scenario could be simplified further if formulated with a particular flavor ansatz. The present work will try to constrain the parameter space for all the three lepton generations simultaneously considering the current experimental updates on $(g - 2)_\ell$ and EDM. However, due to experimental inadequacy, the τ -sector is not at all interesting compared to e and μ . For e -sector, both experimental possibilities (i.e., the results from the Cs and Rb experiments) will be addressed through a common generic formulation. A direct consequence of augmenting the SM with a LQ is opening up the 2-body and 3-body charged lepton flavor violating (CLFV) decay channels and initiating a possibility for the lepton flavor violating Higgs decays [27, 72–74]. However, the experimental upper limits associated with the non-observation of these processes can easily be explained within the considered model by adjusting the lepton-quark couplings in a 3×3 flavor basis, making the parameter space consistent with the CLFV bounds. The paper has been organized as follows. Section 2 introduces the new interactions arising at the TeV scale. In Sect. 3, $(g - 2)_\ell$ and EDM have been defined along with their recent experimental bounds. Section 4 elaborates on the one-loop BSM contributions to the $\ell\ell\gamma$ vertex appearing in the presence of S_1 , whereas in Sect. 5, the allowed parameter space has been analyzed using numerical techniques. Finally, the outcomes have been summarized in Sect. 6.

2 The model: a minimal extension of the SM

The considered model assumes a simple extension of the SM at a NP scale $\Lambda \sim \mathcal{O}(1)$ TeV, where the known particle spectrum gets augmented with a scalar Leptoquark (LQ) of electromagnetic (EM) charge $1/3$ – usually labeled as $S_1 \equiv S_1(\bar{\mathbf{3}}, \mathbf{1}, 1/3)$. Following the notations of Ref. [9], the NP Lagrangian can be cast as,

$$\mathcal{L}_\Lambda = \left[\lambda_L^{ij} \left(\bar{Q}_L^{Cia\beta} \epsilon^{ab} L_L^{jb} \right) S_1^\beta + \lambda_R^{ij} \left(\bar{u}_R^{Ci\beta} S_1^\beta \ell_R^j \right) \right.$$

$$\begin{aligned} &+ \text{h.c.} \Big] + \bar{M}_{S_1}^2 (S_1^\dagger S_1) + \kappa (H^\dagger H) (S_1^\dagger S_1), \\ &= \left[\left\{ \bar{u}_L^{Ci\beta} \left(\mathbb{V}^\dagger \lambda_L \right)^{ij} \ell_L^j - \bar{d}_L^{Ci\beta} \lambda_L^{ij} v_L^j \right\} S_1^\beta \right. \\ &\quad \left. + \lambda_R^{ij} \left(\bar{u}_R^{Ci\beta} S_1^\beta \ell_R^j \right) + \text{h.c.} \right] \\ &\quad + \bar{M}_{S_1}^2 (S_1^\dagger S_1) + \kappa (H^\dagger H) (S_1^\dagger S_1). \end{aligned} \quad (1)$$

Here, the EM charge has been defined as $Q_{\text{EM}} = T_3 + Y$. $Q_L \equiv (u_L \ d_L)^T$ and $L_L \equiv (v_L \ \ell_L)^T$ denote the left-handed quark and lepton doublets, whereas u_R and ℓ_R stand for the right-handed up-type quarks and charged leptons, respectively. The superscript C defines the charge conjugation. The indices $\{i, j\}$ and $\{a, b\}$ define the flavor and $SU(2)$ indices, respectively. β refers to the color index and \mathbb{V} defines the CKM matrix. Equation (1) assumes the down-type quark and charged lepton Yukawas to be in the physical basis. Since neutrinos are insignificant for the low-energy phenomenology, the PMNS matrix has been set to identity. After electroweak symmetry breaking (EWSB) only the SM Higgs acquires a vacuum expectation value (VEV) as,

$$H = \frac{1}{\sqrt{2}} \begin{pmatrix} 0 \\ v + h \end{pmatrix}, \quad (2)$$

where $v = 246$ GeV. Thus, the physical mass of S_1 can be cast as,

$$M_{S_1} = \sqrt{\bar{M}_{S_1}^2 + \frac{\kappa v^2}{2}}, \quad (3)$$

where, \bar{M}_{S_1} is the bare mass term and κ is a dimensionless coupling. In principle, one should consider the kinetic term for S_1 in Eq. (1). However, the NP contributions arising through the interaction of S_1 with the gauge bosons (gluon and photon to be particular)² are irrelevant in the lepton sector. Hence, the kinetic term can be dropped for simplicity.

The NP couplings $\lambda_{L,R}^{ij}$ play a crucial role in describing the low-energy lepton phenomena. At this point, one can easily rotate the Yukawa matrix to the physical basis and constrain the parameter space through the leptonic observables. However, the computational rigor can be reduced through a careful analysis of $\Delta a_\ell = (g - 2)_\ell/2$ and charged lepton flavor violating (CLFV) processes. In Sect. 4, we shall see that Δa_ℓ can be decomposed into two terms – chirality-conserving and chirality-flipping. The former contribution is suppressed by m_ℓ^2 whereas the latter is proportional to the mass of the virtual fermion (here, the SM quarks) appearing in the loop [see Fig. 2]. Therefore, the largest NP contribution to Δa_ℓ corresponds to the t -quark loop, and within

² For a detailed study, see Ref. [31].

the perturbative regime of Yukawa couplings, one can easily neglect the u and c quark contributions to Δa_ℓ considering the mass hierarchy among the three quark generations. Thus, to a good approximation, the mixing among the quarks can be ignored.

Following the above discussion, one may be tempted to assume a minimal flavor structure for enhancing the loop contribution to Δa_ℓ ($\ell = e, \mu, \tau$) as follows:

$$\lambda_{L,R} = \begin{pmatrix} 0 & 0 & 0 \\ 0 & 0 & 0 \\ \lambda_{L,R}^{t,e} & \lambda_{L,R}^{t,\mu} & \lambda_{L,R}^{t,\tau} \end{pmatrix}. \quad (4)$$

However, it can be readily understood that the parameter space presented in Eq. (4) will be strongly constrained through the 2-body and 3-body lepton flavor violating decays. For example, if one sets $|\lambda_{L,R}^{t,e}| \sim \mathcal{O}(1)$, $\text{BR}(\mu \rightarrow e\gamma) < 4.2 \times 10^{-13}$ [75] leads to an upper limit $|\lambda_{L,R}^{t,\mu}| < 10^{-8}$, making it impossible to explain Δa_μ within the assumed parameter space. A similar argument goes for the τ -sector. Therefore, the minimal flavor ansatz should be so chosen that it can maximize the NP contribution to Δa_ℓ while explaining the non-observation of all the CLFV processes in the most economical way. Equation (5) represents the *minimal* Yukawa structure for this simplified model.

$$\lambda_{L,R} = \begin{pmatrix} 0 & 0 & \lambda_{L,R}^{u,\tau} \\ 0 & \lambda_{L,R}^{c,\mu} & 0 \\ \lambda_{L,R}^{t,e} & 0 & 0 \end{pmatrix}. \quad (5)$$

For Eq. (5) one could have equivalently chosen the diagonal line, i.e., $\lambda_{L,R} = \text{diag}(\lambda_{L,R}^{u,e}, \lambda_{L,R}^{c,\mu}, \lambda_{L,R}^{t,\tau})$. Though the phenomenology of μ and τ -sector would remain mostly unchanged, but due to the u -quark mass suppression, this diagonal Yukawa structure would lead to non-perturbative values of $|\lambda_{L,R}^{u,e}|$ for explaining the observed discrepancy in $(g-2)_e$. Note that, the zeros in Eq. (5) are completely from the phenomenological perspective.

3 New physics observables and experimental bounds

The most generic gauge invariant representation for the effective $\ell\ell\gamma$ vertex corresponding to Fig. 1 is given by,

$$\Gamma_{\ell\ell\gamma}^\mu = \gamma^\mu \mathcal{F}_1(q^2) + \left\{ i\mathcal{F}_2(q^2) + \mathcal{F}_4(q^2) \gamma^5 \right\} \left(\frac{\sigma^{\mu\nu} q_\nu}{2m_\ell} \right) + \mathcal{F}_3(q^2) (q^\mu q - q^2 \gamma^\mu) \gamma^5, \quad (6)$$

where $\mathcal{F}_{(1,2,3,4)}$ are the form factors and q represents the photon momentum.

However, in the case of an off-shell photon, there should be additional contributions in Eq. (6). Note that the form factors

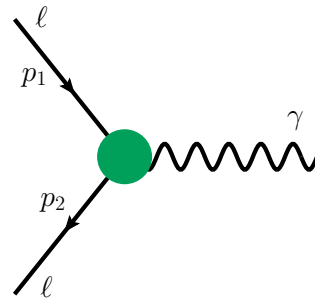


Fig. 1 Effective $\ell\ell\gamma$ vertex. $p_{1,2}$ represent the external momenta, with $q = p_1 - p_2$ being the photon momentum

\mathcal{F}_3 and \mathcal{F}_4 must vanish in any parity-conserving theory (e.g., QED) and can only arise through the diagrams where electroweak (EW) gauge bosons appear as the virtual particles. Thus, the renormalized vertex correction in QED results in [76],

$$\mathcal{F}_1(0) = 0, \quad \mathcal{F}_2(0) = \frac{\alpha_{\text{EM}}}{2\pi}, \quad (7)$$

where $\mathcal{F}_1(0)$ corresponds to the correction in EM charge while $\mathcal{F}_2(0)$ represents the QED contribution to the anomalous magnetic moment of leptons at $\mathcal{O}(\alpha_{\text{EM}})$. However, in the presence of the weak gauge bosons, the $\ell\ell\gamma$ vertex gets modified as [77],³

$$\Gamma_{\text{EW}}^\mu = e \left[\left(1 + \frac{\delta e}{e} \right) \gamma^\mu + \frac{i\sigma^{\mu\nu} q_\nu}{2m_\ell} \left\{ \frac{\alpha_{\text{EM}}}{2\pi} + \mathcal{F}_2^{\text{EW}}(0) \right\} + \frac{\sigma^{\mu\nu} q_\nu}{2m_\ell} \gamma^5 \mathcal{F}_4(0) \right], \quad (8)$$

where δe denotes the sum of the charge correction at one-loop order and the corresponding counterterm. The additional contribution to the anomalous magnetic moment can be parametrized as [79],

$$\mathcal{F}_2^{\text{EW}}(0) = \frac{\mathcal{G}_F m_\ell^2}{8\sqrt{2}\pi^2} \left[\frac{5}{3} + \frac{1}{3}(1 - 4\sin^2\theta_W)^2 + \mathcal{O}\left(\frac{m_\ell^2}{M_W^2}\right) \right], \quad (9)$$

where, \mathcal{G}_F , θ_W , and M_W signify the Fermi constant, weak mixing angle, and mass of the W -boson, respectively. Moreover, considering the leading order (LO) hadronic contribution, one obtains [80],

$$\mathcal{F}_2(0)^{\text{Had}}[\text{LO}] = \left(\frac{\alpha_{\text{EM}}}{\pi\sqrt{3}} \right)^2 \int_{m_\pi^2}^\infty \frac{K(s)}{s} R^{(0)}(s) ds, \quad (10)$$

³ The axial vector coupling associated with the form factor \mathcal{F}_3 vanishes for on-shell photons as a consequence of the Ward identity [78].

where, $K(s)$ stands for the QED kernel function [81] and $R^{(0)}(s)$ represents the ratio of electron–positron bare annihilation cross into the hadrons to the cross section of muon-pair production with center of mass energy \sqrt{s} . However, this leading order hadronic contribution $\mathcal{F}_2(0)^{\text{Had}}[\text{LO}]$ includes a significant amount of uncertainty which might be resolved soon through the updated lattice calculations [47].

The last term in Eq. (8), i.e., $\mathcal{F}_4(0)$ represents the leading order SM contribution to the electric dipole moment (d_ℓ) of leptons. As already mentioned in Sect. 1, despite considering all the SM contributions these leptonic observables exhibit a sharp discrepancy with the experimental results.

3.1 Anomalous magnetic moment

The best available SM prediction for the anomalous magnetic moment of muon is given by $a_\mu^{\text{SM}} = 116591810(43) \times 10^{-11}$ [82], whereas the recent experimental data from Muon $g - 2$ collaboration results in a world average of $a_\mu^{\text{Exp}} = 116592059(22) \times 10^{-11}$ [46], leading to a discrepancy,

$$\Delta a_\mu = a_\mu^{\text{Exp}} - a_\mu^{\text{SM}} = (2.49 \pm 0.48) \times 10^{-9} \quad (5.0\sigma). \quad (11)$$

As discussed, it can be one of the most remarkable signatures of a possible BSM sector. Further, in the context of electrons, experiments indicate a similar anomaly in $(g - 2)_e$. A precision measurement of the fine structure constant through the recoil of Cs^{133} atoms has yielded a notable contradiction between the measured and predicted values of a_e as [50],

$$\Delta a_e^{(\text{Cs})} = a_e^{\text{Exp}(\text{Cs})} - a_e^{\text{SM}} = (-8.8 \pm 3.6) \times 10^{-13} \quad (2.4\sigma). \quad (12)$$

However, for the same a_e a Rubidium based experiment results in [51],

$$\Delta a_e^{(\text{Rb})} = a_e^{\text{Exp}(\text{Rb})} - a_e^{\text{SM}} = (4.8 \pm 3.0) \times 10^{-13} \quad (1.6\sigma). \quad (13)$$

Note that, despite having a significant expectation value, the experimental measurements for Δa_e have large error bars. However, this paper is able to address both of the results for Δa_e , along with the non-zero value of Δa_μ within a common BSM framework.

Unlike the first two generations, measuring the anomalous magnetic moment of τ is extremely challenging due to its short lifetime. Thus, a_τ^{Exp} can only be traced back from the secondary particles produced through the decay of τ . The latest experimental bound (95% CL) can be quoted as [83, 84],

$$-0.052 < a_\tau < 0.013, \quad (14)$$

whereas, the corresponding SM prediction is given by, $a_\tau^{\text{SM}} = 117721(5) \times 10^{-8}$ [85].

3.2 Electric dipole moment

The precision measurement of the electric dipole moment of leptons can be crucial to search for the NP. EDM can be related to the form factor \mathcal{F}_4 as, $d_\ell = e\mathcal{F}_4(0)/m_\ell$, for which the SM predicts $|\mathcal{F}_4^e(0)| < |\mathcal{F}_4^\mu(0)| < |\mathcal{F}_4^\tau(0)| \approx 10^{-23}$ [86–89], i.e., $|d_\tau^{\text{SM}}| \simeq 10^{-37} \text{ e cm}$. It is much smaller than the experimental sensitivity. Thus, any observation of lepton EDM can be treated as a direct evidence of some New Physics interaction. The experimental upper limits for the three lepton generations can be read as [90–92],

$$\begin{aligned} |d_e| &< 0.11 \times 10^{-28} \text{ e cm (90\% CL)}, \\ |d_\mu| &< 1.8 \times 10^{-19} \text{ e cm (95\% CL)}, \\ \text{Re } [d_\tau] &\supset [-0.220, 0.45] \times 10^{-16} \text{ e cm (95\% CL)}, \\ \text{Im } [d_\tau] &\supset [-0.250, 0.08] \times 10^{-16} \text{ e cm (95\% CL)}. \end{aligned} \quad (15)$$

These experimental bounds on Δa_ℓ and d_ℓ will be simultaneously considered to constrain the chosen parameter space for each lepton generation.

3.3 CLFV processes

In general, the CLFV decays are allowed in a S_1 -LQ extension of the SM. However, there is no positive signal from the ongoing experiments [75, 93, 94, 94–101] supporting the lepton flavor violating processes and thus only leads to upper bounds on the Yukawa couplings. Therefore, the non-observation of the 2-body and 3-body CLFV decays can easily be accommodated in this considered model if one follows the Yukawa structure defined by Eq. (5) without any conflict with the experimental data. Thus, the minimal parameter space chosen here is automatically consistent with all the CLFV bounds.

4 BSM contributions to $(g - 2)_\ell$ and EDM

As already stated in Sect. 1, in the presence of a scalar LQ, there can be new contributions to the $\ell\ell\gamma$ vertex at one-loop order. Figure 2a shows the case where the photon couples to the up-type quarks, while Fig. 2b represents the situation when photon touches the S_1 propagator (magenta line). The former will be referred to as Type-1 diagram, while the latter will be called Type-2 for convenience.

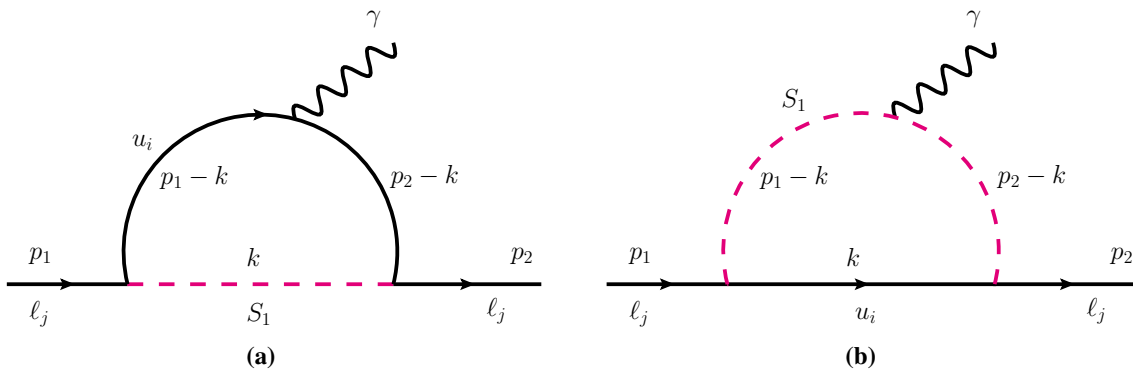


Fig. 2 BSM contributions to the $\ell\ell\gamma$ vertex, where **a** the up-type quarks couple to the photon (Type-1 diagram), and **b** the LQ S_1 couples to the photon (Type-2 diagram). p_1 , p_2 represent the external momenta

4.1 Type-1 diagram

The correction term to $\ell_j \ell_j \gamma$ vertex due to the Type-1 diagram can be computed as,

$$\begin{aligned} \Delta\Gamma_1^\sigma &= i N_C \int \frac{d^4 k}{(2\pi)^4} \left[(-\lambda_L^{ij} P_L + \lambda_R^{ij} P_R) \right. \\ &\quad \times \frac{(\not{p}_2 - \not{k} + m_i)}{(k - p_2)^2 - m_i^2} (\mathcal{Q}_{EM}^i \gamma^\sigma) \frac{(\not{p}_1 - \not{k} + m_i)}{(k - p_1)^2 - m_i^2} \\ &\quad \times \left. \frac{1}{k^2 - M_{S_1}^2} \{ -(\lambda_L^{ij})^* P_R + (\lambda_R^{ij})^* P_L \} \right] \\ &\equiv i \mathcal{Q}_{EM}^i N_C \int \frac{d^4 k}{(2\pi)^4} \left[\frac{\mathcal{N}_1^\sigma}{\mathcal{D}_1} \right]. \end{aligned} \quad (16)$$

Here $N_C = 3$ defines the color degeneracy factor, and $\mathcal{Q}_{EM}^i = 2/3$ represents the EM charge of up-type quarks in the unit of electronic charge e . m_i denotes the up-type quark masses for $i = u, c, t$. The numerator can be rearranged as,

$$\begin{aligned} \mathcal{N}_1^\sigma &= \frac{1}{2} \left[\mathcal{A}_1 \{ (\not{p}_2 - \not{k}) \gamma^\sigma (\not{p}_1 - \not{k}) + m_i^2 \gamma^\sigma \} \right. \\ &\quad + \mathcal{A}_2 m_i \{ (\not{p}_2 - \not{k}) \gamma^\sigma + \gamma^\sigma (\not{p}_1 - \not{k}) \} \\ &\quad + \mathcal{A}_3 \gamma^5 \{ (\not{p}_2 - \not{k}) \gamma^\sigma (\not{p}_1 - \not{k}) + m_i^2 \gamma^\sigma \} \\ &\quad \left. + \mathcal{A}_4 m_i \gamma^5 \{ (\not{p}_2 - \not{k}) \gamma^\sigma + \gamma^\sigma (\not{p}_1 - \not{k}) \} \right], \end{aligned} \quad (17)$$

where,

$$\begin{aligned} \mathcal{A}_1 &= |\lambda_R^{ij}|^2 + |\lambda_L^{ij}|^2, \quad \mathcal{A}_2 = -2 \operatorname{Re}[(\lambda_L^{ij})^* \lambda_R^{ij}], \\ \mathcal{A}_3 &= |\lambda_R^{ij}|^2 - |\lambda_L^{ij}|^2, \quad \mathcal{A}_4 = -2 \operatorname{Im}[(\lambda_L^{ij})^* \lambda_R^{ij}]. \end{aligned} \quad (18)$$

After Feynman parametrization, the denominator can be cast as,

$$\mathcal{D}_1 = n^2 - \Delta_1(x), \quad (19)$$

where $n = k - y p_1 - z p_2$ and $\Delta_1(x) = M_{S_1}^2 [x + \rho_i(1-x)]$. x, y, z are the Feynman parameters and $\rho_i = (m_i/M_{S_1})^2$. This calculation assumes an on-shell photon and the physically viable approximation of $(m_\ell/M_{S_1})^2 \rightarrow 0$. m_ℓ denotes the mass of the SM leptons. Integrating over the loop momentum n , the BSM contributions to the anomalous magnetic moment (Δa_1^ℓ) and electric dipole moment (d_1^ℓ) of the SM leptons can be defined as,

$$\Delta a_1^\ell = \frac{1}{8\pi^2} \left[\mathcal{A}_1 \left(\frac{m_\ell}{M_{S_1}} \right)^2 G_1(\rho_i) + \mathcal{A}_2 \left(\frac{m_\ell m_i}{M_{S_1}^2} \right) G_2(\rho_i) \right], \quad (20)$$

$$d_1^\ell = \frac{e}{8\pi^2} \left[\mathcal{A}_3 \left(\frac{m_\ell}{M_{S_1}^2} \right) G_1(\rho_i) + \mathcal{A}_4 \left(\frac{m_i}{M_{S_1}^2} \right) G_2(\rho_i) \right], \quad (21)$$

where, the functions G_1 and G_2 are given by,

$$\begin{aligned} G_1(w) &= \int_0^1 \left[\frac{x(1-x)^2}{x + (1-x)w} \right] dx \\ &= \frac{2 + 3w - 6w^2 + w^3 + 6w \ln w}{6(1-w)^4}, \\ G_2(w) &= \int_0^1 \left[\frac{(1-x)^2}{x + (1-x)w} \right] dx = \frac{-3 + 4w - w^2 - 2 \ln w}{2(1-w)^3}. \end{aligned} \quad (22)$$

4.2 Type-2 diagram

Figure 2b contributes to the $\ell_j \ell_j \gamma$ vertex as follows.

$$\begin{aligned} \Delta\Gamma_2^\sigma &= i N_C \int \frac{d^4 k}{(2\pi)^4} \left[(-\lambda_L^{ij} P_L + \lambda_R^{ij} P_R) \right. \\ &\quad \times \left. \frac{(\not{k} + m_i)}{k^2 - m_i^2} \cdot \frac{1}{(k - p_1)^2 - M_{S_1}^2} \cdot \mathcal{Q}_{EM}^{S_1} (p_1 + p_2 - 2k)^\sigma \right] \end{aligned}$$

$$\begin{aligned} & \times \frac{1}{(k-p_2)^2 - M_{S_1}^2} \{-(\lambda_L^{ij})^* P_R + (\lambda_R^{ij})^* P_L\}, \\ & \equiv i Q_{EM}^{S_1} N_C \int \frac{d^4 k}{(2\pi)^4} \left[\frac{\mathcal{N}_2^\sigma}{\mathcal{D}_2} \right]. \end{aligned} \quad (23)$$

Here $Q_{EM}^{S_1} = 1/3$ is the EM charge of S_1 . Recasting the numerator of Eq. (23), one gets,

$$\begin{aligned} \mathcal{N}_2^\sigma &= \frac{1}{2} \left[\{\mathcal{A}_1 k + \mathcal{A}_2 m_i\} + \gamma^5 \{\mathcal{A}_3 k + \mathcal{A}_4 m_i\} \right] \\ &\quad \times (p_1 + p_2 - 2k)^\sigma. \end{aligned} \quad (24)$$

Feynman parametrization recasts the denominator as,

$$\begin{aligned} \mathcal{D}_2 &= (k - y p_1 - z p_2)^2 - M_{S_1}^2 \left[x \rho_i + (1-x) \right] \\ &= n^2 - \Delta_2(x). \end{aligned} \quad (25)$$

Thus, the NP contributions to the anomalous magnetic moment and EDM, arising from the Type-2 diagram, can be formulated as,

$$\Delta a_2^\ell = -\frac{1}{16\pi^2} \left[\mathcal{A}_1 \left(\frac{m_\ell}{M_{S_1}} \right)^2 G_3(\rho_i) + \mathcal{A}_2 \left(\frac{m_\ell m_i}{M_{S_1}^2} \right) G_4(\rho_i) \right], \quad (26)$$

$$d_2^\ell = -\frac{e}{16\pi^2} \left[\mathcal{A}_3 \left(\frac{m_\ell}{M_{S_1}^2} \right) G_3(\rho_i) + \mathcal{A}_4 \left(\frac{m_i}{M_{S_1}^2} \right) G_4(\rho_i) \right], \quad (27)$$

where,

$$\begin{aligned} G_3(w) &= \int_0^1 \left[\frac{x(1-x)^2}{xw + (1-x)} \right] dx \\ &= \frac{1 - 6w + 3w^2 + 2w^3 - 6w^2 \ln w}{6(1-w)^4}, \\ G_4(w) &= \int_0^1 \left[\frac{x(1-x)}{xw + (1-x)} \right] dx \\ &= \frac{1 - w^2 + 2w \ln w}{2(1-w)^3}. \end{aligned} \quad (28)$$

Therefore, within this minimally extended BSM framework, the complete NP contribution to the leptonic observables can be defined as,

$$\Delta a_\ell = \Delta a_1^\ell + \Delta a_2^\ell, \quad |d_\ell| = \left| d_1^\ell + d_2^\ell \right|. \quad (29)$$

5 Numerical analysis and results

In this section, we shall try to identify the allowed region of the parameter space through flavor-specific constraints. Δa_ℓ and the experimental upper bound on EDM will be considered simultaneously as the constraining factors for each generation. For completeness, one can enlist the free parameters

of this model as follows:

$$\left\{ M_{S_1}, \lambda_{L,R}^{u,\tau}, \lambda_{L,R}^{c,\mu}, \lambda_{L,R}^{t,e} \right\}.$$

Note that, respecting the LHC constraints at $\sqrt{s} = 13$ TeV one has to choose $M_{S_1} \geq 1.5$ TeV [102–106]. However, the NP couplings can be varied freely within the bounds of perturbative unitarity [107].

Figure 3a shows the allowed parameter space in the $\lambda_{L,R}^{t,e}$ plain for a set of four M_{S_1} values: $M_{S_1} = 1.5$ TeV (violet), 2.0 TeV (golden), 2.5 TeV (sky blue), and 3.0 TeV (red). The depicted region simultaneously satisfies the observed $\Delta a_e^{(Cs)}$ value and the experimental bound on $|d_e|$. However, it is a notable feature of this considered framework that even if one assumes the $\Delta a_e^{(Rb)}$ results instead of Cs, a valid parameter space can be obtained [see Fig. 3b]. Similarly, for the muon sector $\lambda_{L,R}^{c,\mu}$ plain has been constrained through the μ -specific observables, i.e., Δa_μ and $|d_\mu|$ [see Fig. 3c]. Note that, numerically, the same exercise can be repeated for the τ -sector to constrain the $\lambda_{L,R}^{u,\tau}$ region. However, the present experimental sensitivity is inadequate to probe the NP effects to a_τ and d_τ that one can obtain from Fig. 2. Thus, no significant conclusion can be drawn in this case and the entire parameter space is effectively available.

Figure 3 leads to two interesting observations:

- *With increasing M_{S_1} value, the magnitude of the couplings shifts to the higher side.* This particular behavior can be understood by analyzing the M_{S_1} -dependence of Δa_ℓ and d_ℓ for a fixed set of fermion masses. From Eqs. (20)–(21) and (26)–(27) it is clear that there is an overall $M_{S_1}^2$ suppression. However, the complete M_{S_1} -dependence can only be noted by studying the individual variation of the functions $G_{\{1,2,3,4\}}$. Figure 4 shows the variation of the G functions with respect to M_{S_1} . For illustration, $m_\ell = m_\mu = 0.105$ GeV and $m_i = m_c = 1.275$ GeV have been assumed [84]. Figure 4 clearly indicates that G_1 , G_3 , G_4 do not exhibit any notable variation with the increasing M_{S_1} value, while G_2 shows only a slight increment. Thus, to a good approximation, one can conclude that for a given set of quark and lepton masses, Δa_ℓ and $|d_\ell|$ decreases quadratically with M_{S_1} . Therefore, for compensating this suppression, the couplings must rise to match the experimental observations.
- *In Fig. 3a the product $\lambda_{L,R}^{t,e} \times \lambda_{L,R}^{t,e}$ is positive, whereas it flips to a negative value in Fig. 3b.* This is a direct consequence of the oppositely aligned values of $\Delta a_e^{(Cs)}$ and $\Delta a_e^{(Rb)}$. From Fig. 4, one can see that the function G_2 produces the leading contribution over the entire parameter space. The effect is further enhanced due to the chosen flavor ansatz [see Eq. (5)] as it connects the lightest lepton with the heaviest quark and vice versa. Thus, the sign of the

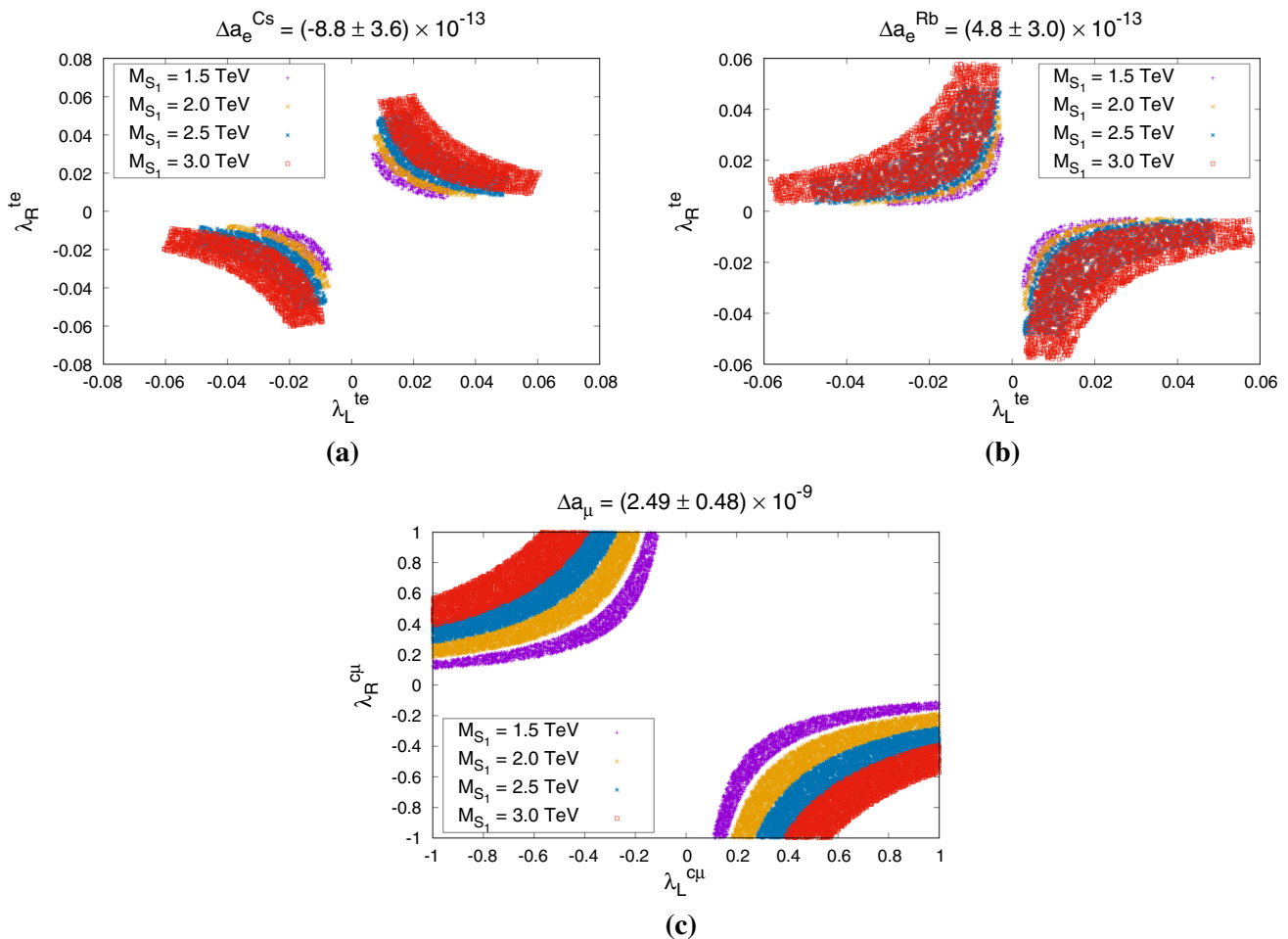


Fig. 3 Allowed parameter space for the first two lepton generations constrained through **a** $\Delta a_e^{(\text{Cs})}$ and $|d_e|$, **b** $\Delta a_e^{(\text{Rb})}$ & $|d_e|$, and **c** Δa_μ and $|d_\mu|$. The four different colors correspond to $M_{S_1} = 1.5 \text{ TeV}$ (violet), 2.0 TeV (golden), 2.5 TeV (sky blue), and 3.0 TeV (red)

term $\mathcal{A}_2 \left(\frac{m_\ell m_i}{M_{S_1}^2} \right) G_2(\rho_i)$ [see Eq. (20)], or to be more specific, the sign of \mathcal{A}_2 effectively decides the sign of Δa_e in the theory. The same argument is valid for the negative values of $\lambda_L^{c,\mu} \times \lambda_R^{c,\mu}$ in Fig. 3c.

6 Conclusions

This paper has considered a minimal extension of the Standard Model with a TeV-scale scalar Leptoquark S_1 transforming as $(\bar{\mathbf{3}}, \mathbf{1}, 1/3)$ under the SM gauge group. In the presence of S_1 , there can be corrections to the $\ell\ell\gamma$ vertex at the one-loop level, which may lead to new physics contributions to the lepton ($g - 2$) and EDM. A particular flavor structure has been chosen to suppress the CLFV processes while enhancing the BSM contributions to other low-energy lepton phenomena. The new one-loop contributions have been computed analytically, followed by a numerical scan to deter-

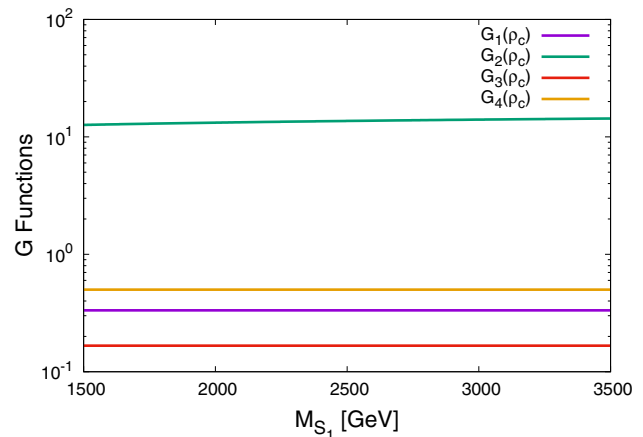


Fig. 4 Variation of G_1 , G_2 , G_3 and G_4 as a function of M_{S_1} for $m_\ell = 0.105 \text{ GeV}$ and $m_i = m_c = 1.275 \text{ GeV}$. Here, $\rho_c = (m_c/M_{S_1})^2$

mine the parameter space allowed under the recent $(g - 2)_\ell$ and EDM constraints for each of the lepton generations. Four different LQ masses have been considered to under-

stand the phenomenological implication of the NP scale on flavor-specific low-energy observables. For the electron sector, viable parameter spaces have been found corresponding to both of the experimental results, i.e., $\Delta a_e^{(\text{Cs})}$ [see Eq. (12)] and $\Delta a_e^{(\text{Rb})}$ [see Eq. (13)]. Note that it is a significant feature of this work that it can explain both positive ($\Delta a_e^{(\text{Rb})}$ and Δa_μ) and negative ($\Delta a_e^{(\text{Cs})}$) discrepancies in the anomalous magnetic moment of leptons by simply rotating the parameter space while keeping the entire scenario consistent with the respective EDM discovery limits. Though the τ -sector has also been analyzed but due to lower experimental sensitivity the complete parameter space is allowed within the perturbative bounds. However, the assumed model structure can explain any future update on a_τ and/or d_τ which can probe the BSM contributions to the τ phenomenology. Collider-based experiments searching for the TeV-scale scalar LQs and/or any experimental update on the low-energy lepton phenomena can be used to test or falsify the proposed framework.

Data Availability Statement This manuscript has no associated data or the data will not be deposited. [Authors' comment: The paper does not use any experimental data that needs to be deposited. All the numerical results presented in this work are self-explanatory and displayed in the figures.]

Open Access This article is licensed under a Creative Commons Attribution 4.0 International License, which permits use, sharing, adaptation, distribution and reproduction in any medium or format, as long as you give appropriate credit to the original author(s) and the source, provide a link to the Creative Commons licence, and indicate if changes were made. The images or other third party material in this article are included in the article's Creative Commons licence, unless indicated otherwise in a credit line to the material. If material is not included in the article's Creative Commons licence and your intended use is not permitted by statutory regulation or exceeds the permitted use, you will need to obtain permission directly from the copyright holder. To view a copy of this licence, visit <http://creativecommons.org/licenses/by/4.0/>.

Funded by SCOAP³. SCOAP³ supports the goals of the International Year of Basic Sciences for Sustainable Development.

References

- ATLAS Collaboration, G. Aad et al., Observation of a new particle in the search for the Standard Model Higgs boson with the ATLAS detector at the LHC. *Phys. Lett. B* **716**, 1–29 (2012). <https://doi.org/10.1016/j.physletb.2012.08.020>. arXiv:1207.7214
- CMS Collaboration, S. Chatrchyan et al., Observation of a new boson at a mass of 125 GeV with the CMS experiment at the LHC. *Phys. Lett. B* **716**, 30–61 (2012). <https://doi.org/10.1016/j.physletb.2012.08.021>. arXiv:1207.7235
- J.C. Pati, A. Salam, Lepton number as the fourth color. *Phys. Rev. D* **10**, 275–289 (1974). <https://doi.org/10.1103/PhysRevD.10.275>. [Erratum: *Phys. Rev. D* **11**, 703 (1975)]
- H. Georgi, S.L. Glashow, Unity of all elementary particle forces. *Phys. Rev. Lett.* **32**, 438–441 (1974). <https://doi.org/10.1103/PhysRevLett.32.438>
- H. Georgi, The state of the art—gauge theories. *AIP Conf. Proc.* **23**, 575–582 (1975). <https://doi.org/10.1063/1.2947450>
- H. Fritzsch, P. Minkowski, Unified interactions of leptons and hadrons. *Ann. Phys.* **93**, 193–266 (1975). [https://doi.org/10.1016/0003-4916\(75\)90211-0](https://doi.org/10.1016/0003-4916(75)90211-0)
- J. Kang, P. Langacker, B.D. Nelson, Theory and phenomenology of exotic isosinglet quarks and squarks. *Phys. Rev. D* **77**, 035003 (2008). <https://doi.org/10.1103/PhysRevD.77.035003>. arXiv:0708.2701
- C. Hati, G. Kumar, N. Mahajan, $\tilde{B} \rightarrow D^{(*)}\tau\bar{\nu}$ excesses in ALRSM constrained from B , D decays and $D^0 - \bar{D}^0$ mixing. *JHEP* **01**, 117 (2016). [https://doi.org/10.1007/JHEP01\(2016\)117](https://doi.org/10.1007/JHEP01(2016)117). arXiv:1511.03290
- I. Doršner, S. Fajfer, A. Greljo, J.F. Kamenik, N. Košnik, Physics of leptoquarks in precision experiments and at particle colliders. *Phys. Rep.* **641**, 1–68 (2016). <https://doi.org/10.1016/j.physrep.2016.06.001>. arXiv:1603.04993
- S. Davidson, D.C. Bailey, B.A. Campbell, Model independent constraints on leptoquarks from rare processes. *Z. Phys. C* **61**, 613–644 (1994). <https://doi.org/10.1007/BF01552629>. arXiv:hep-ph/9309310
- J.L. Hewett, T.G. Rizzo, Much ado about leptoquarks: a comprehensive analysis. *Phys. Rev. D* **56**, 5709–5724 (1997). <https://doi.org/10.1103/PhysRevD.56.5709>. arXiv:hep-ph/9703337
- P. Nath, P. Fileviez Perez, Proton stability in grand unified theories, in strings and in branes. *Phys. Rep.* **441**, 191–317 (2007). <https://doi.org/10.1016/j.physrep.2007.02.010>. arXiv:hep-ph/0601023
- J. Blumlein, E. Boos, A. Kryukov, Leptoquark pair production in hadronic interactions. *Z. Phys. C* **76**, 137–153 (1997). <https://doi.org/10.1007/s002880050538>. arXiv:hep-ph/9610408
- S. Fajfer, N. Košnik, Vector leptoquark resolution of R_K and $R_{D^{(*)}}$ puzzles. *Phys. Lett. B* **755**, 270–274 (2016). <https://doi.org/10.1016/j.physletb.2016.02.018>. arXiv:1511.06024
- R. Barbieri, G. Isidori, A. Pattori, F. Senia, Anomalies in B -decays and $U(2)$ flavour symmetry. *Eur. Phys. J. C* **76**, 67 (2016). <https://doi.org/10.1140/epjc/s10052-016-3905-3>. arXiv:1512.01560
- I. Doršner, S. Fajfer, N. Košnik, I. Nišandžić, Minimally flavored colored scalar in $\tilde{B} \rightarrow D^{(*)}\tau\bar{\nu}$ and the mass matrices constraints. *JHEP* **11**, 084 (2013). [https://doi.org/10.1007/JHEP11\(2013\)084](https://doi.org/10.1007/JHEP11(2013)084). arXiv:1306.6493
- B. Gripaios, M. Nardecchia, S.A. Renner, Composite leptoquarks and anomalies in B -meson decays. *JHEP* **05**, 006 (2015). [https://doi.org/10.1007/JHEP05\(2015\)006](https://doi.org/10.1007/JHEP05(2015)006). arXiv:1412.1791
- D. Bećirević, S. Fajfer, N. Košnik, Lepton flavor nonuniversality in $b \rightarrow s\ell^+\ell^-$ processes. *Phys. Rev. D* **92**, 014016 (2015). <https://doi.org/10.1103/PhysRevD.92.014016>. arXiv:1503.09024
- D. Becirevic, S. Fajfer, N. Košnik, O. Sumensari, Leptoquark model to explain the B -physics anomalies, R_K and R_D . *Phys. Rev. D* **94**, 115021 (2016). <https://doi.org/10.1103/PhysRevD.94.115021>. arXiv:1608.08501
- A. Crivellin, D. Müller, T. Ota, Simultaneous explanation of $R(D^{(*)})$ and $b \rightarrow s\mu^+\mu^-$: the last scalar leptoquarks standing. *JHEP* **09**, 040 (2017). [https://doi.org/10.1007/JHEP09\(2017\)040](https://doi.org/10.1007/JHEP09(2017)040). arXiv:1703.09226
- J.M. Cline, B decay anomalies and dark matter from vectorlike confinement. *Phys. Rev. D* **97**, 015013 (2018). <https://doi.org/10.1103/PhysRevD.97.015013>. arXiv:1710.02140
- L. Di Luzio, M. Nardecchia, What is the scale of new physics behind the B -flavour anomalies? *Eur. Phys. J. C* **77**, 536 (2017). <https://doi.org/10.1140/epjc/s10052-017-5118-9>. arXiv:1706.01868
- T. Mandal, S. Mitra, S. Raz, $R_{D^{(*)}}$ motivated \mathcal{S}_1 leptoquark scenarios: impact of interference on the exclusion limits from LHC data. *Phys. Rev. D* **99**, 055028 (2019). <https://doi.org/10.1103/PhysRevD.99.055028>. arXiv:1811.03561
- U. Aydemir, T. Mandal, S. Mitra, Addressing the $\mathbf{R}_{D^{(*)}}$ anomalies with an \mathbf{S}_1 leptoquark from $\mathbf{SO}(10)$ grand unification. *Phys.*

- Rev. D **101**, 015011 (2020). <https://doi.org/10.1103/PhysRevD.101.015011>. arXiv:1902.08108
25. A. Crivellin, D. Müller, F. Saturnino, Flavor phenomenology of the leptoquark singlet-triplet model. [https://doi.org/10.1007/JHEP06\(2020\)020](https://doi.org/10.1007/JHEP06(2020)020). arXiv:1912.04224
26. P. Asadi, A. Bhattacharya, K. Fraser, S. Homiller, A. Parikh, Wrinkles in the Froggatt–Nielsen mechanism and flavorful new physics. [https://doi.org/10.1007/JHEP10\(2023\)069](https://doi.org/10.1007/JHEP10(2023)069). arXiv:2308.01340
27. K. Cheung, W.Y. Keung, P.Y. Tseng, Leptoquark induced rare decay amplitudes $h \rightarrow \tau^\mp \mu^\pm$ and $\tau \rightarrow \mu\gamma$. Phys. Rev. D **93**, 015010 (2016). <https://doi.org/10.1103/PhysRevD.93.015010>. arXiv:1508.01897
28. R. Mandal, Fermionic dark matter in leptoquark portal. Eur. Phys. J. C **78**, 726 (2018). <https://doi.org/10.1140/epjc/s10052-018-6192-3>. arXiv:1808.07844
29. S.-M. Choi, Y.-J. Kang, H.M. Lee, T.-G. Ro, Lepto-quark portal dark matter. JHEP **10**, 104 (2018). [https://doi.org/10.1007/JHEP10\(2018\)104](https://doi.org/10.1007/JHEP10(2018)104). arXiv:1807.06547
30. A. Mohamadnejad, Accidental scale-invariant Majorana dark matter in leptoquark-Higgs portals. Nucl. Phys. B **949**, 114793 (2019). <https://doi.org/10.1016/j.nuclphysb.2019.114793>. arXiv:1904.03857
31. A. Bhaskar, D. Das, B. De, S. Mitra, Enhancing scalar productions with leptoquarks at the LHC. Phys. Rev. D **102**, 035002 (2020). <https://doi.org/10.1103/PhysRevD.102.035002>. arXiv:2002.12571
32. A. Bhaskar, D. Das, B. De, S. Mitra, A.K. Nayak, C. Neeraj, Leptoquark-assisted singlet-mediated di-Higgs production at the LHC. Phys. Lett. B **833**, 137341 (2022). <https://doi.org/10.1016/j.physletb.2022.137341>. arXiv:2205.12210
33. L. Da Rold, M. Epele, A. Medina, N.I. Mileo, A. Szynkman, Enhancement of the double Higgs production via leptoquarks at the LHC. JHEP **08**, 100 (2021). [https://doi.org/10.1007/JHEP08\(2021\)100](https://doi.org/10.1007/JHEP08(2021)100). arXiv:2105.06309
34. P. Agrawal, U. Mahanta, Leptoquark contribution to the Higgs boson production at the CERN LHC collider. Phys. Rev. D **61**, 077701 (2000). <https://doi.org/10.1103/PhysRevD.61.077701>. arXiv:hep-ph/9911497
35. T. Enkhbat, Scalar leptoquarks and Higgs pair production at the LHC. JHEP **01**, 158 (2014). [https://doi.org/10.1007/JHEP01\(2014\)158](https://doi.org/10.1007/JHEP01(2014)158). arXiv:1311.4445
36. Super-Kamiokande Collaboration, K. Abe et al., Search for proton decay via $p \rightarrow \nu K^+$ using 260 kiloton.year data of super-Kamiokande. Phys. Rev. D **90**, 072005 (2014). <https://doi.org/10.1103/PhysRevD.90.072005>. arXiv:1408.1195
37. I. Dorsner, S. Fajfer, N. Kosnik, Heavy and light scalar leptoquarks in proton decay. Phys. Rev. D **86**, 015013 (2012). <https://doi.org/10.1103/PhysRevD.86.015013>. arXiv:1204.0674
38. W. Buchmuller, D. Wyler, Constraints on su(5)-type leptoquarks. Phys. Lett. B **177**, 377–382 (1986). [https://doi.org/10.1016/0370-2693\(86\)90771-9](https://doi.org/10.1016/0370-2693(86)90771-9)
39. H. Murayama, T. Yanagida, A viable SU(5) GUT with light leptoquark bosons. Mod. Phys. Lett. A **7**, 147–152 (1992). <https://doi.org/10.1142/S0217732392000070>
40. I. Dorsner, P. Fileviez Perez, Unification without supersymmetry: neutrino mass, proton decay and light leptoquarks. Nucl. Phys. B **723**, 53–76 (2005). <https://doi.org/10.1016/j.nuclphysb.2005.06.016>. arXiv:hep-ph/0504276
41. H. Georgi, C. Jarlskog, A new lepton-quark mass relation in a unified theory. Phys. Lett. B **86**, 297–300 (1979). [https://doi.org/10.1016/0370-2693\(79\)90842-6](https://doi.org/10.1016/0370-2693(79)90842-6)
42. P. Fileviez Perez, Renormalizable adjoint SU(5). Phys. Lett. B **654**, 189–193 (2007). <https://doi.org/10.1016/j.physletb.2007.07.075>. arXiv:hep-ph/0702287
43. G. Senjanovic, A. Sokorac, Light leptoquarks in SO(10). Z. Phys. C **20**, 255 (1983). <https://doi.org/10.1007/BF01574858>
44. Muon g-2 Collaboration, B. Abi et al., Measurement of the positive muon anomalous magnetic moment to 0.46 ppm. Phys. Rev. Lett. **126**, 141801 (2021). <https://doi.org/10.1103/PhysRevLett.126.141801>. arXiv:2104.03281
45. Muon g-2 Collaboration, T. Albahri et al., Measurement of the anomalous precession frequency of the muon in the Fermilab Muon g-2 experiment. Phys. Rev. D **103**, 072002 (2021). <https://doi.org/10.1103/PhysRevD.103.072002>. arXiv:2104.03247
46. Muon g-2 Collaboration, D.P. Aguillard et al., Measurement of the positive muon anomalous magnetic moment to 0.20 ppm. <https://doi.org/10.1103/PhysRevLett.131.161802>. arXiv:2308.06230
47. S. Borsanyi et al., Leading hadronic contribution to the muon magnetic moment from lattice QCD. Nature **593**, 51–55 (2021). <https://doi.org/10.1038/s41586-021-03418-1>. arXiv:2002.12347
48. CMD-3 Collaboration, F.V. Ignatov et al., Measurement of the $e^+e^- \rightarrow \pi^+\pi^-$ cross section from threshold to 1.2 GeV with the CMD-3 detector. arXiv:2302.08834
49. G. Colangelo et al., Prospects for precise predictions of a_μ in the Standard Model. arXiv:2203.15810
50. R.H. Parker, C. Yu, W. Zhong, B. Estey, H. Müller, Measurement of the fine-structure constant as a test of the Standard Model. Science **360**, 191 (2018). <https://doi.org/10.1126/science.aap7706>. arXiv:1812.04130
51. L. Morel, Z. Yao, P. Cladé, S. Guellati-Khélifa, Determination of the fine-structure constant with an accuracy of 81 parts per trillion. Nature **588**, 61–65 (2020). <https://doi.org/10.1038/s41586-020-2964-7>
52. A. Djouadi, T. Köhler, M. Spira, J. Tutas, (eb), (et) type leptoquarks at ep colliders. Zeitschrift für Physik C Particles and Fields **46**, 679–685 (1990). <https://doi.org/10.1007/BF01560270>
53. G. Couture, H. König, Bounds on second generation scalar leptoquarks from the anomalous magnetic moment of the muon. Phys. Rev. D **53**, 555–557 (1996). <https://doi.org/10.1103/PhysRevD.53.555>
54. K.-M. Cheung, Muon anomalous magnetic moment and leptoquark solutions. Phys. Rev. D **64**, 033001 (2001). <https://doi.org/10.1103/PhysRevD.64.033001>. arXiv:hep-ph/0102238
55. I. Doršner, S. Fajfer, O. Sumensari, Muon $g - 2$ and scalar leptoquark mixing. [https://doi.org/10.1007/JHEP06\(2020\)089](https://doi.org/10.1007/JHEP06(2020)089). arXiv:1910.03877
56. A. Greljo, P. Stangl, A.E. Thomsen, A model of muon anomalies. Phys. Lett. B **820**, 136554 (2021). <https://doi.org/10.1016/j.physletb.2021.136554>. arXiv:2103.13991
57. K. Kowalska, E.M. Sessolo, Y. Yamamoto, Constraints on charmphilic solutions to the muon $g-2$ with leptoquarks. Phys. Rev. D **99**, 055007 (2019). <https://doi.org/10.1103/PhysRevD.99.055007>. arXiv:1812.06851
58. P. Athron, C. Balázs, D.H.J. Jacob, W. Kotlarski, D. Stöckinger, H. Stöckinger-Kim, New physics explanations of a_μ in light of the FNAL muon $g - 2$ measurement. JHEP **09**, 080 (2021). [https://doi.org/10.1007/JHEP09\(2021\)080](https://doi.org/10.1007/JHEP09(2021)080). arXiv:2104.03691
59. S.-L. Chen, W.-W. Jiang, Z.-K. Liu, Combined explanations of B-physics anomalies, $(g - 2)_{e,\mu}$ and neutrino masses by scalar leptoquarks. Eur. Phys. J. C **82**, 959 (2022). <https://doi.org/10.1140/epjc/s10052-022-10920-x>. arXiv:2205.15794
60. S. Saad, Combined explanations of $(g - 2)_\mu$, $R_{D^{(*)}}$, $R_{K^{(*)}}$ anomalies in a two-loop radiative neutrino mass model. Phys. Rev. D **102**, 015019 (2020). <https://doi.org/10.1103/PhysRevD.102.015019>. arXiv:2005.04352
61. V. Gherardi, D. Marzocca, E. Venturini, Low-energy phenomenology of scalar leptoquarks at one-loop accuracy. JHEP **01**, 138 (2021). [https://doi.org/10.1007/JHEP01\(2021\)138](https://doi.org/10.1007/JHEP01(2021)138). arXiv:2008.09548

62. A. Bhaskar, A.A. Madathil, T. Mandal, S. Mitra, Combined explanation of W-mass, muon g-2, RK(*) and RD(*) anomalies in a singlet-triplet scalar leptoquark model. *Phys. Rev. D* **106**, 115009 (2022). <https://doi.org/10.1103/PhysRevD.106.115009>. arXiv:2204.09031
63. S. Parashar, A. Karan, Avnish, P. Bandyopadhyay, K. Ghosh, Phenomenology of scalar leptoquarks at the LHC in explaining the radiative neutrino masses, muon g-2, and lepton flavor violating observables. *Phys. Rev. D* **106**, 095040 (2022). <https://doi.org/10.1103/PhysRevD.106.095040>. arXiv:2209.05890
64. D. Zhang, Radiative neutrino masses, lepton flavor mixing and muon $g - 2$ in a leptoquark model. *JHEP* **07**, 069 (2021). [https://doi.org/10.1007/JHEP07\(2021\)069](https://doi.org/10.1007/JHEP07(2021)069). arXiv:2105.08670
65. E. Coluccio Leskow, G. D'Ambrosio, A. Crivellin, D. Müller, $(g - 2)\mu$, lepton flavor violation, and Z decays with leptoquarks: correlations and future prospects. *Phys. Rev. D* **95**, 055018 (2017). <https://doi.org/10.1103/PhysRevD.95.055018>. arXiv:1612.06858
66. R. Mandal, A. Pich, Constraints on scalar leptoquarks from lepton and kaon physics. *JHEP* **12**, 089 (2019). [https://doi.org/10.1007/JHEP12\(2019\)089](https://doi.org/10.1007/JHEP12(2019)089). arXiv:1908.11155
67. N. Ghosh, S.K. Rai, T. Samui, Collider signatures of a scalar leptoquark and vectorlike lepton in light of muon anomaly. *Phys. Rev. D* **107**, 035028 (2023). <https://doi.org/10.1103/PhysRevD.107.035028>. arXiv:2206.11718
68. W. Altmannshofer, S. Gori, H.H. Patel, S. Profumo, D. Tucker, Electric dipole moments in a leptoquark scenario for the B -physics anomalies. *JHEP* **05**, 069 (2020). [https://doi.org/10.1007/JHEP05\(2020\)069](https://doi.org/10.1007/JHEP05(2020)069). arXiv:2002.01400
69. W. Dekens, J. de Vries, M. Jung, K.K. Vos, The phenomenology of electric dipole moments in models of scalar leptoquarks. *JHEP* **01**, 069 (2019). [https://doi.org/10.1007/JHEP01\(2019\)069](https://doi.org/10.1007/JHEP01(2019)069). arXiv:1809.09114
70. K. Fuyuto, M. Ramsey-Musolf, T. Shen, Electric dipole moments from CP-violating scalar leptoquark interactions. *Phys. Lett. B* **788**, 52–57 (2019). <https://doi.org/10.1016/j.physletb.2018.11.016>. arXiv:1804.01137
71. I. Bigaran, R.R. Volkas, Reflecting on chirality: CP-violating extensions of the single scalar-leptoquark solutions for the $(g - 2)_{e,\mu}$ puzzles and their implications for lepton EDMs. *Phys. Rev. D* **105**, 015002 (2022). <https://doi.org/10.1103/PhysRevD.105.015002>. arXiv:2110.03707
72. W.-F. Chang, S.-C. Liou, C.-F. Wong, F. Xu, Charged lepton flavor violating processes and scalar leptoquark decay branching ratios in the colored Zee-Babu model. *JHEP* **10**, 106 (2016). [https://doi.org/10.1007/JHEP10\(2016\)106](https://doi.org/10.1007/JHEP10(2016)106). arXiv:1608.05511
73. T. Husek, K. Monsalvez-Pozo, J. Portoles, Constraints on leptoquarks from lepton-flavour-violating tau-lepton processes, in *JHEP*. (2022), p.165. [https://doi.org/10.1007/JHEP04\(2022\)165](https://doi.org/10.1007/JHEP04(2022)165). arXiv:2111.06872
74. L. Delle Rose, C. Marzo, L. Marzola, Simplified leptoquark models for precision $l_i \rightarrow l_f \gamma$ experiments: two-loop structure of $O(\alpha_s Y^2)$ corrections. *Phys. Rev. D* **102**, 115020 (2020). <https://doi.org/10.1103/PhysRevD.102.115020>. arXiv:2005.12389
75. MEG Collaboration, A.M. Baldini et al., Search for the lepton flavour violating decay $\mu^+ \rightarrow e^+ \gamma$ with the full dataset of the MEG experiment. *Eur. Phys. J. C* **76**, 434 (2016). <https://doi.org/10.1140/epjc/s10052-016-4271-x>. arXiv:1605.05081
76. J. Schwinger, On quantum-electrodynamics and the magnetic moment of the electron. *Phys. Rev.* **73**, 416–417 (1948). <https://doi.org/10.1103/PhysRev.73.416>
77. W. Hollik, Electroweak radiative corrections, M_Z , M_W , and the heavy top. *Adv. Ser. Direct. High Energy Phys.* **10**, 1–57 (1992). https://doi.org/10.1142/9789814503587_0001
78. J.C. Ward, An identity in quantum electrodynamics. *Phys. Rev.* **78**, 182 (1950). <https://doi.org/10.1103/PhysRev.78.182>
79. R. Jackiw, S. Weinberg, Weak interaction corrections to the muon magnetic moment and to muonic atom energy levels. *Phys. Rev. D* **5**, 2396–2398 (1972). <https://doi.org/10.1103/PhysRevD.5.2396>
80. M. Gourdin, E. De Rafael, Hadronic contributions to the muon g-factor. *Nucl. Phys. B* **10**, 667–674 (1969). [https://doi.org/10.1016/0550-3213\(69\)90333-2](https://doi.org/10.1016/0550-3213(69)90333-2)
81. S.J. Brodsky, E. De Rafael, Suggested boson-lepton pair couplings and the anomalous magnetic moment of the muon. *Phys. Rev.* **168**, 1620–1622 (1968). <https://doi.org/10.1103/PhysRev.168.1620>
82. T. Aoyama et al., The anomalous magnetic moment of the muon in the Standard Model. *Phys. Rep.* **887**, 1–166 (2020). <https://doi.org/10.1016/j.physrep.2020.07.006>. arXiv:2006.04822
83. DELPHI Collaboration, J. Abdallah et al., Study of tau-pair production in photon-photon collisions at LEP and limits on the anomalous electromagnetic moments of the tau lepton. *Eur. Phys. J. C* **35**, 159–170 (2004). <https://doi.org/10.1140/epjc/s2004-01852-y>. arXiv:hep-ex/0406010
84. Particle Data Group Collaboration, R.L. Workman et al., Review of particle physics. *PTEP* **2022**, 083C01 (2022). <https://doi.org/10.1093/ptep/ptac097>
85. S. Eidelman, M. Passera, Theory of the tau lepton anomalous magnetic moment. *Mod. Phys. Lett. A* **22**, 159–179 (2007). <https://doi.org/10.1142/S0217732307022694>. arXiv:hep-ph/0701260
86. M.J. Booth, The electric dipole moment of the W and electron in the Standard Model. arXiv:hep-ph/9301293
87. U. Mahanta, Dipole moments of the τ lepton as a sensitive probe for physics beyond the standard model. *Phys. Rev. D* **54**, 3377–3381 (1996). <https://doi.org/10.1103/PhysRevD.54.3377>
88. Y. Yamaguchi, N. Yamanaka, Large long-distance contributions to the electric dipole moments of charged leptons in the standard model. *Phys. Rev. Lett.* **125**, 241802 (2020). <https://doi.org/10.1103/PhysRevLett.125.241802>
89. Y. Yamaguchi, N. Yamanaka, Quark level and hadronic contributions to the electric dipole moment of charged leptons in the standard model. *Phys. Rev. D* **103**, 013001 (2021). <https://doi.org/10.1103/PhysRevD.103.013001>
90. ACME Collaboration, V. Andreev et al., Improved limit on the electric dipole moment of the electron. *Nature* **562**, 355–360 (2018). <https://doi.org/10.1038/s41586-018-0599-8>
91. Muon (g-2) Collaboration, G.W. Bennett et al., An improved limit on the muon electric dipole moment. *Phys. Rev. D* **80**, 052008 (2009). <https://doi.org/10.1103/PhysRevD.80.052008>. arXiv:0811.1207
92. Belle Collaboration, K. Inami et al., Search for the electric dipole moment of the tau lepton. *Phys. Lett. B* **551**, 16–26 (2003). [https://doi.org/10.1016/S0370-2693\(02\)02984-2](https://doi.org/10.1016/S0370-2693(02)02984-2). arXiv:hep-ex/0210066
93. A.M. Baldini et al., MEG upgrade proposal. arXiv:1301.7225
94. T. Aushev et al., Physics at super B factory. arXiv:1002.5012
95. BaBar Collaboration, B. Aubert et al., Searches for lepton flavor violation in the decays $\tau^\pm \rightarrow e^\pm \gamma$ and $\tau^\pm \rightarrow \mu^\pm \gamma$. *Phys. Rev. Lett.* **104**, 021802 (2010). <https://doi.org/10.1103/PhysRevLett.104.021802>. arXiv:0908.2381
96. A. Blondel et al., Research proposal for an experiment to search for the decay $\mu \rightarrow eee$. arXiv:1301.6113
97. U. Bellgardt, G. Otter, R. Eichler, L. Felawka, C. Niebuhr, H. Walter et al., Search for the decay $\mu^+ \rightarrow e^+ e^+ e^-$. *Nucl. Phys. B* **299**, 1–6 (1988). [https://doi.org/10.1016/0550-3213\(88\)90462-2](https://doi.org/10.1016/0550-3213(88)90462-2)
98. K. Hayasaka et al., Search for lepton flavor violating tau decays into three leptons with 719 million produced tau+tau-pairs. *Phys. Lett. B* **687**, 139–143 (2010). <https://doi.org/10.1016/j.physletb.2010.03.037>. arXiv:1001.3221
99. ATLAS Collaboration, G. Aad et al., Search for the Higgs boson decays $H \rightarrow ee$ and $H \rightarrow e\mu$ in pp collisions at $\sqrt{s} = 13$ TeV with the ATLAS detector. *Phys. Lett. B* **801**,

- 135148 (2020). <https://doi.org/10.1016/j.physletb.2019.135148>. arXiv:1909.10235
100. ATLAS Collaboration, G. Aad et al., Searches for lepton-flavour-violating decays of the Higgs boson in $\sqrt{s} = 13$ TeV pp collisions with the ATLAS detector. *Phys. Lett. B* **800**, 135069 (2020). <https://doi.org/10.1016/j.physletb.2019.135069>. arXiv:1907.06131
101. CMS Collaboration, A.M. Sirunyan et al., Search for lepton flavour violating decays of the Higgs boson to $\mu\tau$ and $e\tau$ in proton–proton collisions at $\sqrt{s} = 13$ TeV. *JHEP* **06**, 001 (2018). [https://doi.org/10.1007/JHEP06\(2018\)001](https://doi.org/10.1007/JHEP06(2018)001). arXiv:1712.07173
102. CMS Collaboration, A.M. Sirunyan et al., Search for pair production of first-generation scalar leptoquarks at $\sqrt{s} = 13$ TeV. *Phys. Rev. D* **99**, 052002 (2019). <https://doi.org/10.1103/PhysRevD.99.052002>. arXiv:1811.01197
103. ATLAS Collaboration, G. Aad et al., Search for pairs of scalar leptoquarks decaying into quarks and electrons or muons in $\sqrt{s} = 13$ TeV pp collisions with the ATLAS detector. *JHEP* **10**, 112 (2020). [https://doi.org/10.1007/JHEP10\(2020\)112](https://doi.org/10.1007/JHEP10(2020)112). arXiv:2006.05872
104. ATLAS Collaboration, M. Aaboud et al., Searches for scalar leptoquarks and differential cross-section measurements in dilepton-dijet events in proton–proton collisions at a centre-of-mass energy of $\sqrt{s} = 13$ TeV with the ATLAS experiment. *Eur. Phys. J. C* **79**, 733 (2019). <https://doi.org/10.1140/epjc/s10052-019-7181-x>. arXiv:1902.00377
105. CMS Collaboration, A.M. Sirunyan et al., Search for pair production of second-generation leptoquarks at $\sqrt{s} = 13$ TeV. *Phys. Rev. D* **99**, 032014 (2019). <https://doi.org/10.1103/PhysRevD.99.032014>. arXiv:1808.05082
106. CMS Collaboration, A.M. Sirunyan et al., Search for third-generation scalar leptoquarks decaying to a top quark and a τ lepton at $\sqrt{s} = 13$ TeV. *Eur. Phys. J. C* **78**, 707 (2018). <https://doi.org/10.1140/epjc/s10052-018-6143-z>. arXiv:1803.02864
107. L. Allwicher, P. Arnan, D. Barducci, M. Nardecchia, Perturbative unitarity constraints on generic Yukawa interactions. *JHEP* **10**, 129 (2021). [https://doi.org/10.1007/JHEP10\(2021\)129](https://doi.org/10.1007/JHEP10(2021)129). arXiv:2108.00013